# NATURAL CONVECTION BOUNDARY LAYER FLOW ALONG A SPHERE EMBEDDED IN A POROUS MEDIUM FILLED WITH A NANOFLUID

A.M. RASHAD

*Department of Mathematics, Faculty of Science, Aswan University, 81528, Egypt. E-mail: am_rashad@yahoo.com*

***Abstract*— A boundary-layer analysis is presented for the natural convection boundary layer flow about a sphere embedded in a porous medium filled with a nanofluid using Brinkman-Forchheimer-Darcy extended model. The model used for the nanofluid incorporates the effects of Brownian motion and thermophoresis. The governing partial differential equations are transformed into a set of nonsimilar equations and solved numerically by an efficient implicit, iterative, finite-difference method. Comparisons with previously published work are performed and excellent agreement is obtained. A parametric study of the physical parameters is conducted and a representative set of numerical results for the velocity, temperature, and nanoparticles volume fraction profiles as well as the local skin-friction coefficient, local Nusselt and Sherwood numbers is illustrated graphically to show interesting features of the solutions.**

***Keywords*— Natural convection; porous medium; sphere; nanofluid; thermophoresis.**

## I. INTRODUCTION

Convective heat transfer from fixed or rotating bodies embedded in porous media has been extensively studied by many investigators owing to its many applications in engineering, such as post accidental heat removal in nuclear reactors, solar collectors, drying processes, heat exchangers, geothermal energy recovery, and crude oil extraction, ground water pollution, thermal energy storage, building construction, flow through filtering media, modeling of packed sphere beds, ground water pollution and filtration processes, to name just a few of these applications. However, representative studies in this area may be found in the monographs by Vafai (2000), Pop and Ingham (2001), Ingham and Pop (2002) and Nield and Bejan (2006) have summarized the importance of both boundary and inertia effects in porous media. Yih (2000) examined the non-Darcy MHD natural convection flow over a permeable sphere in a porous medium. EL-Hakiem and Rashad (2007) investigated the non-Darcy natural convection flow over a vertical cylinder saturated porous medium. EL-Kabeir *et al.* (2007) studied the natural convection from a sphere embedded in a variable porosity porous medium. EL-Kabeir *et al.* (2008) have studied the effect of thermal radiation on the combined heat and mass transfer on MHD non-Darcy free convection about a horizontal cylinder embedded in a saturated porous medium.

Nanofluids are prepared by dispersing solid nanoparticles in fluids such as water, oil, or ethylene glycol. These fluids represent an innovative way to increase thermal conductivity and, therefore, heat transfer. Unlike heat transfer in conventional fluids, the exceptionally high thermal conductivity of nanofluids provides for exceptional heat transfer, a unique feature of nanofluids. Advances in device miniaturization have necessitated heat transfer systems that are small in size, light mass, and high-performance. Several authors have tried to establish convective transport models for nanofluids. An innovative technique for improving heat transfer by using ultra fine solid particles in the fluids has been used extensively during the last several years. The term nanofluid refers to these kinds of fluids by suspending nano-scale particles in the base fluid and has been introduced by Choi (1995). Use of metallic nanoparticles with high thermal conductivity will increase the effective thermal conductivity of these types of fluid remarkably. Buongiorno (2006) found that the nanoparticle absolute velocity can be written as the sum of the base fluid velocity and the slip velocity. Nield and Kuznetsov (2009) have studied the classical problem of free convection boundary layer flow of a Newtonian fluid past a vertical flat plate in a porous medium saturated by a nanofluid. Chamkha *et al.* (2011a) have studied the natural convection past a sphere embedded in a porous medium saturated by a nanofluid. A similarity analysis for the problem of a steady boundary-layer flow of a nanofluid on an isothermal stretching circular cylindrical surface is investigated by Gorla *et al.* (2011a). Gorla *et al.* (2011b) have also analyzed mixed convective boundary layer flow over a vertical wedge embedded in a porous medium saturated with a nanofluid. Chamkha *et al.* (2011b) analyzed the effect of melting on unsteady hydromagnetic flow of a nanofluid past a stretching sheet. The problem of natural convection boundary layer of a non-Newtonian fluid about vertical cone embedded in a porous medium saturated with nanofluid has been performed by Rashad *et al.* (2011). Khan and Aziz (2011) have analyzed double-diffusive natural convective boundary layer flow over a vertical plate embedded in a porous medium saturated with a nanofluid. Chamkha *et al.* (2012a, 2013a) presented the effect of radiation on mixed convection over a wedge and cone embedded in a porous medium filled with a nanofluid. Cheng (2012) considered free convection boundary layer flow over a horizontal cylinder of elliptic cross section in porous media saturated by a nanofluid. Uddin *et al.* (2012) have considered a numerical solution for free convection boundary layer flow from a heated upward facing horizontal flat plate embedded in

a porous medium filled by a nanofluid. Chamkha and Rashad (2012) studied the natural convection from a vertical permeable cone in nanofluid saturated porous media for uniform heat and nanoparticles volume fraction fluxes. Chamkha *et al.* (2012b) have investigated the effect of radiation on boundary-layer flow of a nanofluid on a continuously moving or fixed permeable surface. Chamkha *et al.* (2013b) have analyzed the transient natural convection flow of a nanofluid over a vertical cylinder. The problem of natural convection boundary-layer flow adjacent to a vertical cylinder embedded in a thermally stratified nanofluid saturated non-Darcy porous medium is investigated by Rashad *et al.* (2013).

The present work has been undertaken in order to analyze the natural convection boundary layer flow about a sphere embedded in a porous medium filled with a nanofluid using Brinkman-Forchheimer-Darcy extended model. The effects of Brownian motion and thermophoresis are included for the nanofluid. Numerical solutions of the boundary layer equations are obtained and discussion is provided for several values of the nanofluid parameters governing the problem.

## II. MATHEMATICAL FORMULATION

Consider steady natural convection boundary-layer flow from along a sphere embedded in non-Darcy porous medium filled with a nanofluid. The model used for the nanofluid incorporates the effects of Brownian motion and thermophoresis. The sphere surface is maintained at a constant temperature $T_w$ and a constant nano-particle volume fraction $C_w$ and the ambient temperature and nano-particle volume fraction far away from the surface of the sphere $T_\infty$ and $C_\infty$ are assumed to be uniform. For $T_w > T_\infty$ and $C_w > C_\infty$ an upward flow is induced as a result of the thermal and nano-particle volume fraction buoyancy effects. The schematics of the problem under consideration and the coordinate system are shown in Fig. 1. The porous medium is assumed to be uniform, isotropic and in local thermal equilibrium with the fluid. All fluid properties are assumed to be constant. Under the Boussinesq and boundary-layer approximations, the governing equations for this problem can be written as: The fluid is assumed to Newtonian, incompressible and viscous. All fluid properties are assumed to be constant except the density variation in the buoyancy force term of the x-momentum equation. Upon treating the fluid-saturated porous medium as a continuum (see, Vafai and Tien, 1981), including the non-Darcian boundary and inertia effects, and assuming that the Boussinesq approximation is valid, the boundary-layer form of mass, momentum, temperature and nanoparticles volume fraction can be written as (see, Huang and Chen, 1987; and Nazar and Amin 2002)

$$\frac{\partial (RU)}{\partial X} + \frac{\partial (RV)}{\partial Y} = 0 , \tag{1}$$

$$\rho_f \left( U \frac{\partial U}{\partial X} + V \frac{\partial U}{\partial Y} \right) = g \sin\left( \frac{X}{a} \right)$$

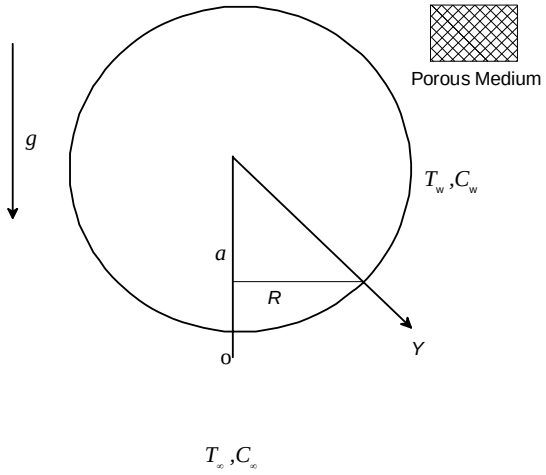


**Fig. 1.** Flow model and coordinate system

$$\left( (1 - C_\infty) \rho_{f\infty} \beta (T - T_\infty) - (\rho_P - \rho_{f\infty})(C - C_\infty) \right) + \mu \frac{\partial^2 U}{\partial Y^2} - \frac{\mu}{K} U - K^* U^2 , \tag{2}$$

$$U \frac{\partial T}{\partial X} + V \frac{\partial T}{\partial Y} = \alpha \frac{\partial^2 T}{\partial Y^2} + \tau \left[ D_B \frac{\partial C}{\partial Y} \frac{\partial T}{\partial Y} + \frac{D_T}{T_\infty} \left( \frac{\partial T}{\partial Y} \right)^2 \right], \tag{3}$$

$$\frac{1}{\varphi} \left( U \frac{\partial C}{\partial X} + V \frac{\partial C}{\partial Y} \right) = D_B \frac{\partial^2 C}{\partial Y^2} + \left( \frac{D_T}{T_\infty} \right) \frac{\partial^2 T}{\partial Y^2} . \tag{4}$$

The boundary conditions for this problem are defined as follows:

$$Y = 0 : U = 0 \;\; V = 0 \;\; T = T_w \;\; C = C_w ,$$
$$Y \to \infty : U = 0 \;\; T = T_\infty \;\; C = C_\infty , \tag{5}$$

where $R(i)=a \sin(X/a)$ is the radial distance from symmetric axis to surface of the sphere, $a$ is the radius of the sphere, $U$ and $V$ are the velocity components along $X$ and $Y$ axes, respectively, $T$ is the temperature, $C$ is the nanoparticle concentration, g is the acceleration due to gravity, $K$ is the permeability of porous medium, $K^*$ is the empirical constant associated with the Forchheimer porous inertia term, $\phi$ is the porosity, $\alpha = k/(\rho c)_f$ is the thermal diffusivity of the fluid and $\tau = (\rho c)_p/(\rho c)_f$. Further, $\rho f_\infty$ is the density of the base fluid and $\rho$, $\mu$, $k$ and $\beta$ are the density, viscosity, thermal conductivity and volumetric thermal expansion coefficient of the nanofluid, while $\rho_p$ is the density of the nanoparticles, $(\rho c)_f$ is the heat capacity of the fluid and $(\rho c)_p$ is the effective heat capacity of the nanoparticle material. The coefficients that appear in Eqs. (3)-(4) are the Brownian diffusion coefficient $D_B$, the thermophoretic diffusion coefficient $D_T$. For, details of the derivation of Eqs. (1)-(5), one can refer the papers by Buongiorno (2006) and Nield and Kuznetsov (2009). The above equations are further non-dimensionalised using the new variables:

$$x=\frac{X}{a},\quad y=\frac{Y}{a}Gr^{1/4},\quad u=\frac{a}{\upsilon Gr^{1/2}}U,\quad v=\frac{a}{\upsilon Gr^{1/4}}V,$$
$$Gr=\frac{(1-C_\infty)\rho_{f\infty}^2 g\beta(T_w-T_\infty)a^3}{\mu^2},\theta=\frac{T-T_\infty}{T_w-T_\infty},$$
$$\phi=\frac{C-C_\infty}{C_w-C_\infty},r=a\sin(x/a), \tag{6}$$

where $v=\mu./\rho f_\infty$ is the kinematic viscosity coefficient and $Gr$ is the Grashof number, $\theta$ and $\phi$ are the nondimensional functions of temperature and nanoparticle concentration, respectively. Substituting the variables (6) into Eqs. (1)-(4) lead to the following nondimensional equations:

$$\frac{\partial(ru)}{\partial x}+\frac{\partial(rv)}{\partial y}=0, \tag{7}$$

$$u\frac{\partial u}{\partial x}+v\frac{\partial u}{\partial y}=\frac{\partial^2 u}{\partial y^2}+\frac{\sin x}{x}(\theta-Nr\phi)-\frac{1}{Da}u-\Gamma u^2, \tag{8}$$

$$u\frac{\partial\theta}{\partial x}+v\frac{\partial\theta}{\partial y}=\frac{1}{\Pr}\frac{\partial^2\theta}{\partial y^2}+Nb\frac{\partial\phi}{\partial y}\frac{\partial\theta}{\partial y}+Nt\left(\frac{\partial\theta}{\partial y}\right)^2, \tag{9}$$

$$u\frac{\partial\phi}{\partial x}+v\frac{\partial\phi}{\partial y}=\frac{1}{Le}\frac{\partial^2\phi}{\partial y^2}+\frac{Nt}{Le\ Nb}\frac{\partial^2\theta}{\partial y^2}. \tag{10}$$

The boundary conditions for this problem are defined as follows:

$$y=0:\quad u=0\quad v=0\quad \theta=1\quad \phi=1,$$
$$y\to\infty:\quad u=0\quad \theta=0\quad \phi=0, \tag{11}$$

where $Da$ and $\Gamma$ are the Darcy and Forchheimer numbers, respectively (reflect the permeability of porous medium and inertia effects), $Nr$ is the buoyancy ratio parameter, $Nb$ is the Brownian motion parameter, $Nt$ is the thermophoresis parameter, Pr is the Prandtl number and $Le$ is the Lewis number, which are defined respectively as;

$$Da=\frac{KGr^{1/2}}{a^2},\Gamma=K^*a,Nr=\frac{(\rho_p-\rho_{f\infty})(C_w-C_\infty)}{\rho_{f\infty}\beta(T_w-T_\infty)(1-C_\infty)},$$
$$Nb=\frac{\varphi(\rho c)_p D_B(C_w-C_\infty)}{(\rho c)_f\upsilon},$$
$$Nt=\frac{\varphi(\rho c)_p D_T(T_w-T_\infty)}{(\rho c)_f\upsilon T_\infty},\Pr=\frac{\upsilon}{\alpha},Le=\frac{\upsilon}{\varphi D_B}. \tag{12}$$

To solve Eqs. (7)-(9), subject to the boundary conditions (10), we assume the following transformations:

$$\psi=xr(x)f(x,y),\ \theta=\theta(x,y),\ \phi=\phi(x,y), \tag{13}$$

where $\psi$ is the stream function defined in the usual way as $u=(1/r)\partial\psi/\partial y$ and $v=-(1/r)\partial\psi/\partial x$, therefore the continuity equation is identically satisfied. In addition the velocities components are Substituting Eqs. (13) into Eqs. (7)-(11) the transformed equations take the following form:

$$f'''+\left(1+\frac{x}{\tan x}\right)ff''+\frac{\sin x}{x}(\theta-Nr\phi)-\frac{1}{Da}f'$$
$$-(1+x\Gamma)(f')^2=x\left(f'\frac{\partial f'}{\partial x}-f''\frac{\partial f}{\partial x}\right), \tag{14}$$

$$\frac{1}{\Pr}\theta''+Nb\phi'\theta'+\left(1+\frac{x}{\tan x}\right)f\theta'+Nt\theta'^2=$$
$$x\left(f'\frac{\partial\theta}{\partial x}-\theta'\frac{\partial f}{\partial x}\right), \tag{15}$$

$$\phi''+Le\left(1+\frac{x}{\tan x}\right)f\phi'+\frac{Nt}{Nb}\theta''=$$
$$Le\ x\left(f'\frac{\partial\phi}{\partial x}-\phi'\frac{\partial f}{\partial x}\right). \tag{16}$$

along with the boundary conditions;

$$y=0:\quad f'=0\quad f=0\quad \theta=1\quad \phi=1$$
$$y\to\infty:\quad f'=0\quad \theta=0\quad \phi=0, \tag{17}$$

where the primes indicate partial differentiation with respect to $y$. It can be seen that near the lower stagnation point of the sphere, i.e., when x≈0, Eqs. (14)-(16) reduce to the following ordinary differential equations:

$$f'''+2ff''+(\theta-Nr\phi)-\frac{1}{Da}f'-(f')^2=0, \tag{18}$$

$$\frac{1}{\Pr}\theta''+Nb\phi'\theta'+2f\theta'+Nt\theta'^2=0, \tag{19}$$

$$\phi''+2Lef\phi'+\frac{Nt}{Nb}\theta''=0 \tag{20}$$

subject to the boundary conditions

$$y=0:\quad f'=0\quad f=0\quad \theta=1\quad \phi=1,$$
$$y\to\infty:\ f'=0\ \ \theta=0\ \ \phi=0. \tag{21}$$

In practical applications, the physical quantities of principal interest are the shearing stress and the rate of heat transfer in terms of the skin-friction coefficient $C_f$, Nusselt number $Nu$ and Sherwood number respectively, which can be written as;

$$C_f=\frac{Gr^{-3/4}a^2}{\upsilon}\tau_w,Nu=-\frac{aGr^{-1/4}q_w}{k(T_w-T_\infty)},$$
$$Sh=-\frac{aGr^{-1/4}m_w}{D(C_w-C_\infty)}, \tag{22}$$

where

$$\tau_w=\left(\frac{\partial U}{\partial Y}\right)_{Y=0},q_w=\left(\frac{\partial T}{\partial Y}\right)_{Y=0},m_w=\left(\frac{\partial C}{\partial Y}\right)_{Y=0}. \tag{23}$$

Using the non-dimensional variables (6), and (13) and the boundary conditions (17) into Eqs. (22) and (23), one can obtain the following:

$$C_f(x)=xf''(x,0),Nu(x)=-\theta'(x,0),$$
$$Sh(x)=-\phi'(x,0). \tag{24}$$

## III. NUMERICAL METHOD

The non-similar Eqs. (14)-(16) are linearized and then descritized using three points central difference quotients with variable step sizes in the $y$ direction and using two-point backward difference formulas in the $x$ direction with a constant step size. The resulting equations form a tri-diagonal system of algebraic equations that can be solved by the well-known Thomas algorithm (see Blottmer, 1977). The solution process starts at $x$=0, where Eqs. (18)-(20) are solved, and then marches for-

ward using the solution at the previous line of constant $x$ until it reaches the desired value of $x$ (=120$^o$ in this case). Due to the nonlinearities of the equations, an iterative solution with successive over- or under-relaxation techniques is required. The convergence criterion required that the maximum absolute error between two successive iterations be $10^{-6}$. The computational domain was made of 196 grids in the $y$ direction and 1,000 grids in the $x$ direction. A starting step size of 0.001 in the $y$ direction with an increase of 1.0375 times the previous step size and a constant step size in the $x$ direction of 0.0021 were found to give very accurate results. The maximum value of $y$, which represented the ambient conditions, was assumed to be 35. The step sizes employed were arrived at after performing numerical experimentations to assess grid independence and ensure accuracy of the results.

The accuracy of the aforementioned numerical method was validated by direct comparison with the numerical results reported earlier by Huang and Chen (1987) and Nazar and Amin (2002) for various values of $x$, at $Nr = Nb = Nt = 0$ and $\Gamma$=Da$^{-1}$=0 (in the absence of the nanofluid parameters, permeability of porous medium and inertia effects) at Pr=0.7. Table 1 presents the results of this comparison. It can be seen from this table that excellent agreement between the results exists. This favorable comparison lends confidence in the numerical results to be reported in the next section.

## IV. RESULTS AND DISCUSSION

In this section, a representative set of graphical results for the dimensionless velocity $f'(x,y)$, temperature $\theta(x,y)$, and nanoparticles volume fraction $\phi(x,y)$ profiles, as well as the local skin-friction coefficient $C_f(x)$, local Nusselt number $Nu(x)$ (reciprocal of rate of heat transfer), and the local Sherwood number $Sh(x)$ (reciprocal of rate of mass transfer)is presented and discussed for various values namely; Darcy number Da, Forchheimer number $\Gamma$, nanofluid buoyancy ratio Nr, Brownian motion parameter Nb, thermophoresis parameter Nt, Lewis number Le and the circumferential position parameter $x$.

Figures 2-4 illustrate the effects of the Darcy number Da and Lewis number Le on velocity $f'(x,y)$, temperature $\theta(x,y)$, and nanoparticles volume fraction $\phi(x,y)$ profiles, respectively. Physically, the presence of a porous medium in the flow presents resistance to flow. Thus, the resulting resistive force tends to retard the motion of the fluid along the sphere surface and causes increases in its temperature and volume fraction. This is shown in Figs. 2-4, by the increases in the velocity profiles and decreases in the values of both the temperature and concentration as the Darcy number $Da$ increases. On other hand, it is noticed that an increase in the values of Le results in acceleration of the flow represented by increases in the velocity profiles because of the reduction in the nanoparticle buoyancy effect. Moreover, as Le increases both the nanofluid temperature and volume fraction profiles and its thermal and nanoparticle concentration boundary layer thickness decrease.

**Table 1.** Comparison of values of Nu at Pr=0.7 with Huang and Chen (1987) and Nazar and Amin (2002) for Da$^{-1}$=0.0, $\Gamma$=0.0, Nr=0, Nb=0.0 and Nt=0.0.

| $x$ | Huang and Chen (1987) | Nazar and Amin (2002) | Present results |
|---|---|---|---|
| 0$^o$ | 0.4576 | 0.4574 | 0.4577 |
| 10$^o$ | 0.4563 | 0.4565 | 0.4568 |
| 20$^o$ | 0.4532 | 0.4533 | 0.4540 |
| 30$^o$ | 0.4480 | 0.4480 | 0.4486 |
| 40$^o$ | 0.4407 | 0.4405 | 0.4410 |
| 50$^o$ | 0.4312 | 0.4308 | 0.4315 |
| 60$^o$ | 0.4194 | 0.4189 | 0.4197 |
| 70$^o$ | 0.4053 | 0.4046 | 0.4054 |
| 80$^o$ | 0.3886 | 0.3879 | 0.3889 |
| 90$^o$ | 0.3694 | 0.3684 | 0.3694 |

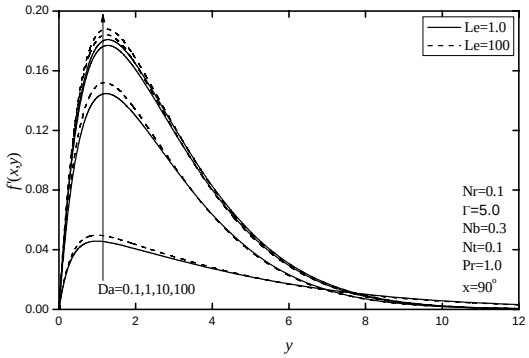


Fig. 2: Effects of Da and Le on the velocity profiles

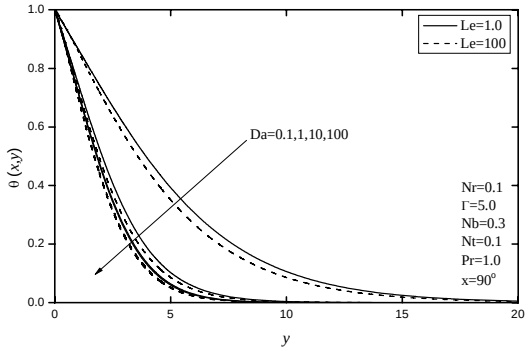


Fig. 3: Effects of Da and Le on the temperature profiles

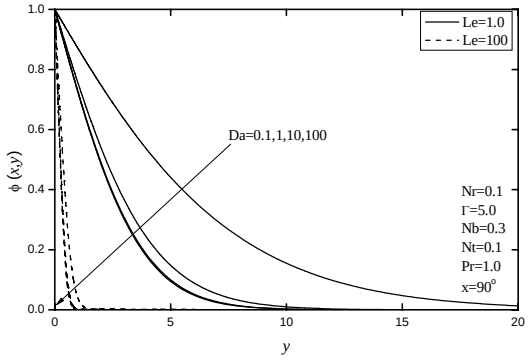


Fig. 4: Effects of Da and Le on the volume fraction profiles

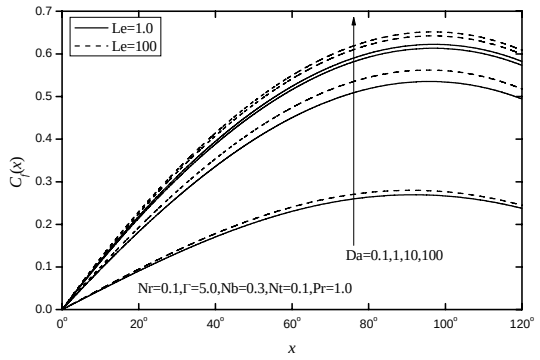


Fig. 5: Effects of Da and Le on the local skin-friction coefficient

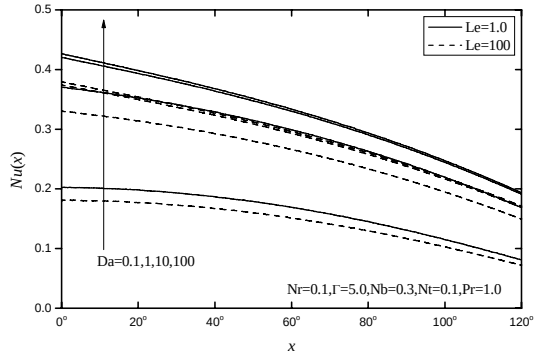


Fig. 6: Effects of Da and Le on the local Nusselt number

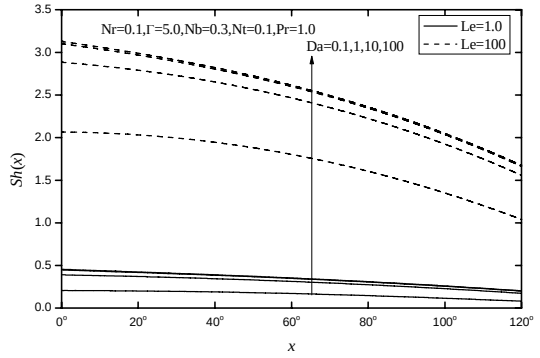


Fig. 7: Effects of Da and Le on the local Sherwood number

Figures 5-7 display the variations of the local skin-friction coefficient $C_f(x)$ (reciprocal of shear stress), local Nusselt number $Nu(x)$ (reciprocal of rate of heat transfer), and the local Sherwood number $Sh(x)$ (reciprocal of rate of mass transfer) due to changes in the values of *Da* and Le, respectively. In general, as the circumferential position parameter $x$ increases, the skin-friction coefficient rises considerably whereas the opposite behavior happens with the local Nusselt and Sherwood numbers. Also, from the above observation, as seen from Figs. 3 and 4, for a given value of the Lewis number Le, increasing the Darcy number *Da* causes the temperature and volume fraction at the sphere surface to decrease at every circumferential position $\xi$. This behavior results in increases in both the local Nusselt and Sherwood numbers according to Eqs. (18) and (19). Also, as *Da* increases, the wall slope of the velocity profile $f''(\xi,0)$ increases and, based on Eq. (17), its value increases. However, both $C_f(x)$ and $Sh(x)$ are enhanced, whereas $Nu(x)$ is reduced as the Lewis number Le increases. This is associated with the decreases in the nanoparticle concentration boundary layer as Le increases as discussed earlier. Thus, the influence of the Lewis number is to reduce the heat transfer rate and enhance either of skin friction and nanoparticle mass transfer rate.

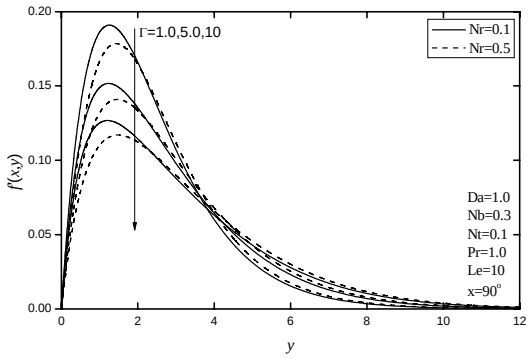


Fig. 8: Effects of Γ and Nr on the velocity profiles

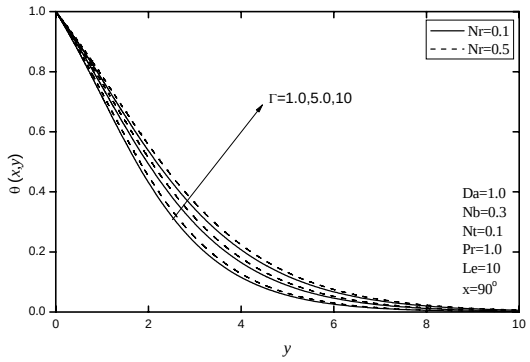


Fig. 9: Effects of Γ and Nr on the temperature profiles

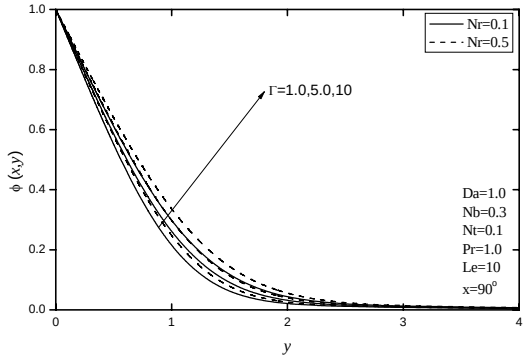


Fig. 10: Effects of Γ and Nr on the volume fraction profiles

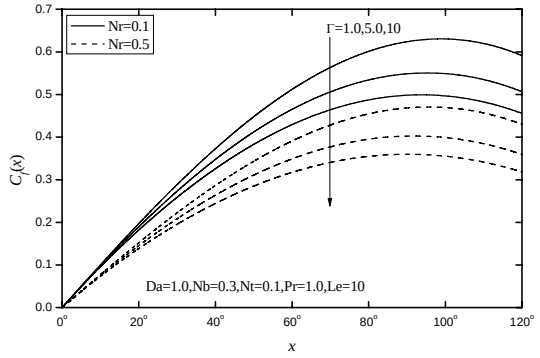


Fig. 11: Effects of Γ and Nr on the local the skin-friction coefficient

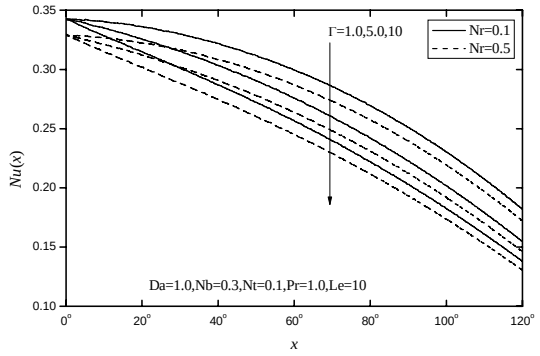


Fig. 12: Effects of Γ and Nr on the local Nusselt number

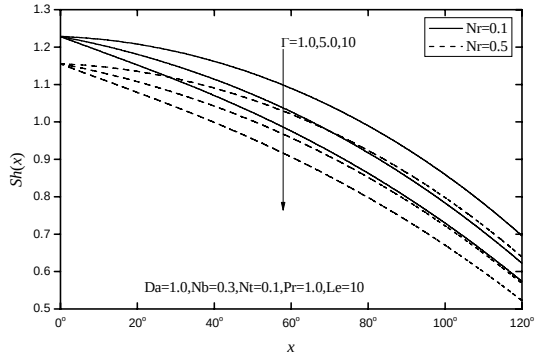


Fig. 13: Effects of Γ and Nr on the local Sherwood number

Figures 8-10 show the effects of Forchheimer number Γ and nanoparticle buoyancy ratio Nr on the velocity $f'(x,y)$, temperature $\theta(x,y)$ and nanoparticles volume fraction $\phi(x,y)$ profiles, respectively. In these figures, it is predicted that Forchheimer number Γ is found to characterize the fluid inertia effect which presents an obstacle to flow causing the flow to move slower and both the nanofluid temperature and volume fraction to increase. Hence, an increase in Γ, causes an increase in the thermal and nanoparticle concentration boundary layer thickness and a decrease in the momentum boundary layer thickness. However, It is shown that the velocity profiles decreases near the wall and showing the opposite trend far away from the wall with the increase of nanoparticle buoyancy ratio *Nr*. On contrast, both the temperature and nanoparticle volume fraction profiles increase with increasing values of *Nr*. These increases in both the temperature and volume fraction values are followed by corresponding slight increases in both thermal and nanoparticle concentration boundary layer thickness. These behaviors are clearly shown in Figs. 8-10.

In Figs. 11-13, the effects of Γ and Nr on the local skin-friction coefficient $C_f(x)$, local Nusselt number $Nu(x)$, and local Sherwood number $Sh(x)$, respectively. For a given buoyancy ratio *Nr*, increasing the Forchheimer number Γ is found to have significant effect on both the skin-friction coefficient and local Nusselt number. As Γ increases, the fluid motion in the boundary layer is decelerated causing enhancement in the momentum boundary layer and hence, in the thermal and nanoparticle concentration boundary layer thickness. Consequently, the velocity gradient and hence, the skin-friction coefficient decrease with increasing values of Γ. Consequently, all the local skin-friction coefficient, local Nusselt and Sherwood numbers are reduced with increasing values of Γ. In addition, a similar behavior is noticed where all of these physical parameters increase as buoyancy ratio Nr. This is due to the fact that the increase of buoyancy ratio Nr has a tendency to decelerate the flow along the sphere surface which filled with nanofluids. This behavior in the flow velocity is accompanied by slight increases in the nanofluid temperature and volume fraction as Nr increases.

Figures 14-16 depict the effects of the Brownian motion parameter Nb and thermophoresis parameter Nt on velocity $f'(x,y)$, temperature $\theta(x,y)$, and nanoparticles volume fraction $\phi(x,y)$ profiles, respectively. It is seen that the increasing the Brownian motion parameter Nb produces increases in either of the velocity or temperature profiles with significant decrease on the volume fraction profiles, while increasing the thermophoresis parameter Nt leads to increase the velocity, temperature and volume fraction profiles.

Figures 17-19 show the influences of the Brownian motion parameter Nb and the thermophoresis parameter Nt on the local skin friction coefficient $C_f(x)$, local Nusselt number $\mathrm{Nu}(x)$ and local Sherwood number $\mathrm{Sh}(x)$, respectively. In nanofluid systems, owing to the size of the nanoparticles, Brownian motion takes place, and this can enhance the heat transfer properties. This is due to the fact that the Brownian diffusion promotes heat conduction. The nanoparticles increase the sphere surface area for heat transfer. A nanofluid is a two phase fluid where the nanoparticles move randomly and raise the energy exchange rates. However, the Brownian motion decreases nanoparticles diffusion. The enhancement in the local Sherwood number as Brownian motion parameter Nb changes is relatively small. Therefore, as noted before that, the effect of the Brownian motion parameter Nb is to increase the velocity and temperature profiles while its volume fraction decreases. This yields

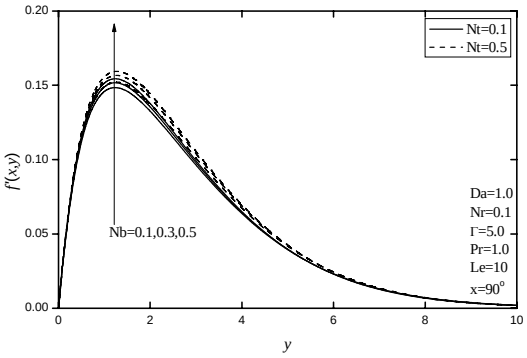


Fig. 14: Effects of Nb and Nt on the velocity profiles

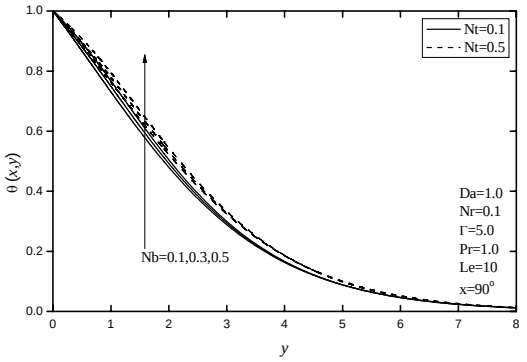


Fig. 15: Effects of Nb and Nt on the temperature profiles

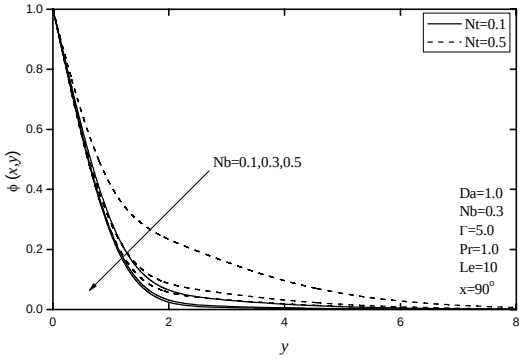


Fig. 16: Effects of Nb and Nt on the volume fraction profiles

reduction in the local Nusselt number and enhancement in both the skin friction coefficient and local Sherwood number.

On the other hand, it can be seen that the thermophoresis parameter Nt appears in thermal and nanoparticles concentration boundary layer equations. This is consistence with the well known fact that it is coupled with the temperature function and plays a strong role in determining the diffusion of heat and nanoparticles concentration in the boundary layer. Thus, an increasing in the values of the thermophoresis parameter Nt has a tendency to decrease in the local Nusselt number whereas this trend is reversed in both the local skin friction coefficient and local Sherwood number.

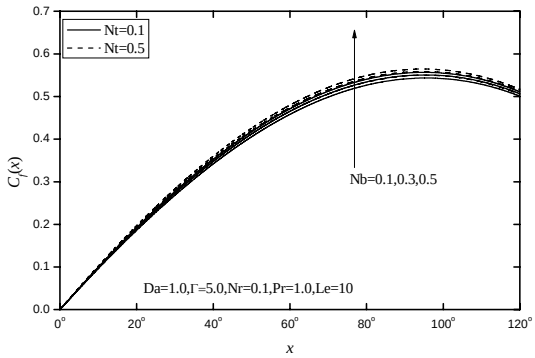


Fig. 17: Effects of Nb and Nt on the local skin-friction coefficient

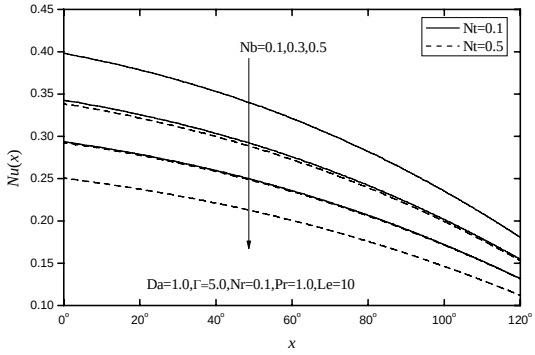


Fig. 18: Effects of Nb and Nt on the local Nusselt number

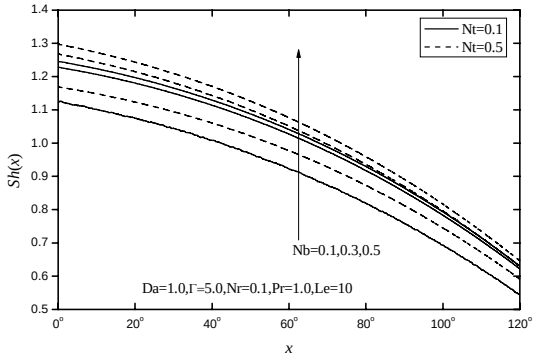


Fig. 18: Effects of Nb and Nt on the local Sherwood number

## V. CONCLUSIONS

This work considered the natural convection laminar boundary layer flow along a sphere embedded in a porous medium filled with a nanofluid using the Brinkman-Forchheimer-Darcy extended model were studied. The model used for the nanofluid incorporates the effects of Brownian motion and thermophoresis. The governing equations were formulated and transformed into a set of non-similar equations which are solved numerically by an accurate, implicit, iterative, finite-difference method. Comparisons with previously published work were performed and excellent agreement was obtained. Calculations were carried out for a wide range of values

of the pertinent parameters to examine the results from this method. Graphical results for the velocity, temperature and nanoparticles volume fraction profiles as well as the local skin-friction coefficient and local Nusselt and Sherwood numbers are presented and discussed for various parametric conditions. It was found that both the local Nusselt and Sherwood numbers raised due to increases in Darcy number (reflect the permeability of porous medium). However, they both reduced due to increases in either the Forchheimer number (reflect inertia effects), buoyancy ratio or the circumferential position. Also, increases in the values of either of Brownian motion parameter, thermophoresis parameter or Lewis number produced decreases in the local Nusselt number and increases in the local Sherwood number. Finally, the skin-friction coefficient was enhanced as either of Darcy number, Lewis number, Brownian motion parameter, thermophoresis parameter or the circumferential position increased, while, the opposite behavior was predicted as the buoyancy ratio or Forchheimer number was increased. It is hoped that the present work will serve as a motivation for future experimental work which seems to be lacking at the present time.

## ACKNOWLEDGEMENTS

The author is very thankful to the reviewers for their constructive comments which have improved significantly the quality of the paper.

## REFERENCES

Blottner, F.G., "Finite-difference methods of solution of the boundary-layer equations," *AIAA Journal*, **8,** 193-205 (1970).

Buongiorno, J., "Convective transport in nanofluids," *ASME J. Heat Transfer*, **128**, 240-250 (2006).

Chamkha, A.J. and A.M. Rashad, "Natural convection from a vertical permeable cone in nanofluid saturated porous media for uniform heat and nanoparticles volume fraction fluxes," *Int. J. Numerical Methods for Heat and Fluid Flow*, **22**, 1073-1085 (2012).

Chamkha, A.J., R.S.R. Gorla and K. Ghodeswar, "Non-similar solution for natural convective boundary layer flow over a sphere embedded in a porous medium saturated with a nanofluid," *Transport in Porous Media*, **86,** 13-22 (2011a).

Chamkha, A.J., A.M. Rashad and E. Al-Meshaiei, "Melting effect on unsteady hydromagnetic flow of a nanofluid past a stretching sheet," *Int. J. Chemical Reactor Engineering*, **9**, 1-23 (2011b).

Chamkha, A.J., S. Abbasbandy, A.M. Rashad and K. Vajravelu, "Radiation effects on mixed convection over a wedge embedded in a porous medium filled with a nanofluid," *Transport in Porous Medium*, **91**, 261-279 (2012a).

Chamkha, A.J., M. Modather, S.M.M. EL-Kabeir and A.M. Rashad, "Radiative effects on boundary-layer flow of a nanofluid on a continuously moving or fixed permeable surface," *Recent Patents on Mechanical Engineering*, **5**, 176-183 (2012b).

Chamkha, A.J., S. Abbasbandy, A.M. Rashad and K. Vajravelu, "Radiation effects on mixed convection about a cone embedded in a porous medium filled with a nanofluid," *Meccanica*, **48**, 275-285 (2013a).

Chamkha, A.J., A.M. Rashad and A.M. Aly, "Transient natural convection flow of a nanofluid over a vertical cylinder," *Meccanica*, **48**, 71-81 (2013b).

Cheng, C.Y., "Free convection boundary layer flow over a horizontal cylinder of elliptic cross section in porous media saturated by a nanofluid," *Int. Comm. Heat Mass Transfer*, **39**, 931-936 (2012).

Choi, S.U.S., "Enhancing thermal conductivity of fluids with nanoparticle," in: D.A. Siginer, H.P. Wang (Eds.), *Developments and Applications of Non-Newtonian Flows*, ASME FED, 231/MD **66**, 99-105 (1995).

EL-Hakiem, M.A. and A.M. Rashad, "Effect of radiation on non-Darcy free convection from a vertical cylinder embedded in a fluid-saturated porous medium with a temperature-dependent viscosity," *J. Porous Media*, **10**, 209-218 (2007).

EL-Kabeir, S.M.M., M.A. EL-Hakiem and A.M. Rashad, "Group Method Analysis Of Combined Heat And Mass Transfer By MHD Non-Darcy Non-Newtonian Natural Convection Adjacent To Horizontal Cylinder In A Saturated Porous Medium," *Applied Mathematical Modelling*, **32**, 2378-2395 (2008).

EL-Kabeir, S.M.M., M.A. El-Hakiem and A.M. Rashad, "Natural convection from a permeable sphere embedded in a variable porosity porous medium due to thermal dispersion," *Nonlinear Analysis: Modelling and Control*, **12**, 345-357 (2007).

Gorla, R.S.R., A.J. Chamkha and A.M. Rashad, "Mixed convective boundary layer flow over a vertical wedge embedded in a porous medium saturated with a nanofluid: Natural convection dominated regime," *Journal of Nanoscale Research Letters*, **6**, 1-9 (2011a).

Gorla, R.S.R., S.M.M. EL-Kabeir and A.M. Rashad, "Heat transfer in the boundary layer on a stretching circular cylinder in a nanofluid," *Journal of Thermophysics and Heat Transfer*, **25**, 183-186 (2011b).

Huang, M. J. and C.K. Chen, "Laminar free convection from a sphere with blowing and suction," *J. Heat Transfer*, **109**, 529-532 (1987).

Ingham, D.B. and Pop, I. (Eds.), *Transport Phenomena in Porous Media, Pergamon*, Oxford (2002).

Khan, W.A. and A. Aziz, "Double-diffusive natural convective boundary layer flow in a porous medium saturated with a nanofluid over a vertical plate: Prescribed surface heat, solute and nanoparticle fluxes," *Int. J. Therm. Sci.*, **50**, 2154-2160 (2011).

Nazar, R. and N. Amin, "Free convection boundary layer on an isothermal sphere in a micropolar flu-

id," *Int. Commun. Heat Mass Transfer*, **29**, 377-386 (2002).

Nield, D.A. and A. Bejan, *Convection in Porous Media*, third Ed., Springer, New York (2006).

Nield, D.A. and A.V. Kuznetsov, "The Cheng-Minkowycz problem for natural convective boundary layer flow in a porous medium saturated by a nanofluid," *Int. J. Heat Mass Transfer*, **52**, 5792-5795 (2009).

Pop, I. and D.B. Ingham, *Convective Heat Transfer: mathematical and computational modelling of viscous fluids and porous media*, Pergamon, Oxford (2001).

Rashad, A.M., M.A. EL-Hakiem and M.M.M. Abdou, "Natural convection boundary layer of a non-Newtonian fluid about a permeable vertical cone embedded in a porous medium saturated with a nanofluid," *Computers and Mathematics with Applications*, **62**, 3140-3151 (2011).

Rashad, A.M., S. Abbasbandy and A.J. Chamkha, "Non-Darcy natural convection from a vertical cylinder embedded in a thermally stratified and nanofluid-saturated porous media," *ASME Journal of Heat Transfer*, doi: 10.1115/1.4025559, In press (2013).

Uddin, M.J., W.A. Khan and A.I.M. Ishmail, "Free convection boundary layer flow from a heated upward facing horizontal flat plate embedded in a porous medium filled by a nanofluid with convective boundary condition," *Transp. Porous Media*, **92**, 867-881 (2012).

Vafai, K. and C.L. Tien, "Boundary and inertia effects on flow and heat transfer in porous media," *Int. J. Heat Mass Transfer*, **24**, 195-203 (1981).

Vafai, K., (Ed.), *Handbook of Porous Media*, Marcel Dekker, Marcel (2000).

Yih, K.A., "Viscous and Joule heating effects on non-Darcy MHD natural convection flow over a permeable sphere in porous media with internal heat generation," *Int. Commun. Heat Mass Transfer*, **27**, 591-600 (2000).

**Received: June 22, 2013**
**Accepted: October 23, 2013**
**Recommended by Subject Editor: Walter Ambrosini**